

Ultraviolet and Infrared Photodissociation of $\text{Si}^+(\text{C}_6\text{H}_6)_n$ and $\text{Si}^+(\text{C}_6\text{H}_6)_n\text{Ar}$ Clusters

J. B. Jaeger, E. D. Pillai, T. D. Jaeger, and M. A. Duncan*

Department of Chemistry, University of Georgia, Athens, Georgia 30602-2556

Received: November 13, 2004; In Final Form: January 26, 2005

Ion–molecule complexes of the form $\text{Si}^+(\text{C}_6\text{H}_6)_n$ and $\text{Si}^+(\text{C}_6\text{H}_6)_n\text{Ar}$ are produced by laser vaporization in a pulsed nozzle cluster source. These clusters are mass-selected and studied with ultraviolet (355 nm) photodissociation and resonance-enhanced infrared photodissociation spectroscopy in the C–H stretch region of benzene. In the UV, $\text{Si}^+(\text{C}_6\text{H}_6)_n$ clusters ($n = 1–5$) fragment to produce the $\text{Si}^+(\text{C}_6\text{H}_6)$ mono-ligand species, suggesting that this ion has enhanced relative stability. IR photodissociation of $\text{Si}^+(\text{C}_6\text{H}_6)_n$ complexes occurs by the elimination of benzene, while $\text{Si}^+(\text{C}_6\text{H}_6)_n\text{Ar}$ complexes lose Ar. Resonances reveal C–H vibrational bands in the 2900–3300 cm^{-1} region characteristic of the benzene ligand with shifts caused by the silicon cation bonding. The IR spectra confirm that the major component of the $\text{Si}^+(\text{C}_6\text{H}_6)$ ions studied have the π -complex structure rather than the isomeric insertion products suggested previously.

Introduction

Silicon ions play an important role in atmospheric chemistry,^{1,2} astrophysics,^{3–5} and semiconductor plasmas.⁶ Because of their widespread importance, silicon-containing ions have been investigated in numerous mass spectrometry experiments. Ion–molecule reactions and collision-induced dissociation experiments have investigated reaction pathways and bonding energetics.^{7–15} While these studies have been insightful, there are few examples of the spectroscopy of silicon-containing ions. Si^+ has no electronic states at low energy, and therefore electronic spectroscopy on $\text{Si}^+(\text{L})_n$ complexes is problematic. However, recent infrared photodissociation spectroscopy experiments have been demonstrated for silicon ion–molecule complexes, providing useful structural information.^{16,17} In the present study, we examine $\text{Si}^+(\text{benzene})_n$ complexes with both ultraviolet and infrared photodissociation measurements. These experiments probe the stability of these ions and their structures.

Cation–benzene complexes of various metals have been studied extensively by experiment and theory.^{18–36} These studies have focused on transition metals or main group metals, but there are relatively few studies of silicon–benzene ions.^{7–9,12,13,15} $\text{Si}^+(\text{C}_6\text{H}_6)_n$ complexes are potentially important in astrophysics because benzene is a precursor of polycyclic aromatic hydrocarbons (PAHs) and both silicon and PAHs are highly abundant in the interstellar/stellar media.^{37–40} The adduct ion SiC_6H_6^+ was first reported by Allen and Lampe in collisional studies of Si^+ with benzene.⁷ Bohme and co-workers used the selected ion flow tube method to investigate reactions of Si^+ with benzene that formed the adduct ion.⁸ Further studies by this group included reactions of SiC_6H_6^+ with other small molecules. From the reaction products generated, they concluded that the silicon cation is located above the benzene ring in a π -bonded configuration. A joint study by the Schwarz and Bohme groups in 1992 used chemical ionization and neutralization–reionization mass spectrometry experiments in conjunction with ab initio calculations.¹⁰ On the basis of the results of theory, they proposed three possible isomers for SiC_6H_6^+ , including a π -complex, a C–H insertion complex, and a ring insertion

complex. Their experiments found evidence for the π -complex and the C–H insertion complex but not for the ring insertion isomer. The binding energy (D_e) of Si^+ to benzene in the π -complex was calculated to be 1.92 eV compared to 1.68 eV in the C–H insertion complex. The calculated structure for the π -complex does not have the ion on the C_6 axis, but rather it is in a position nearly above one carbon of the benzene ring, lowering the overall symmetry to C_s . The perturbation of the π -system causes the nearest hydrogen atom to be bent out of the plane of the benzene ring by about 10 degrees. Collisional dissociation of SiC_6H_6^+ produced fragment ions such as SiC_6H_5^+ , SiC_4H_4^+ , and SiC_4H_3^+ , consistent with the strong binding of silicon to the organic framework of benzene.⁹ In later work, Beauchamp and co-workers studied ion–molecule reactions of SiC_6H_6^+ in an FT-ICR mass spectrometer,¹¹ and they found evidence for all three of the isomers proposed by the Schwarz group. Another FT-ICR mass spectrometry study using a laser vaporization cluster source was performed by Dunbar and co-workers, revealing two reaction pathways for $\text{Si}^+ + \text{C}_6\text{H}_6$.¹² In the first, SiC_6H_6^+ is formed by radiative association, accounting for 15% of the products. Second, $\text{SiC}_6\text{H}_5^+ + \text{H}$ were formed by condensation with hydrogen atom elimination, accounting for 85% of the products. Additionally, the study observed no cluster formation between $\text{Si}^+(\text{C}_6\text{H}_6)$ and benzene, ruling out the possibility of a stable “sandwich” structure. This research group placed a lower-limit on the binding energy of 2.2 eV for the SiC_6H_6^+ complex. More recently, Tang and co-workers studied reactions between silicon ions and benzene.¹⁵ They observed both association complexes, $\text{Si}(\text{C}_6\text{H}_6)_n^+$ where $n = 1$ and 2, and dissociative complexes, $\text{Si}(\text{C}_5\text{H}_5)^+$, $\text{Si}(\text{C}_7\text{H}_5)^+$, and $\text{Si}(\text{C}_9\text{H}_5)^+$. This group also performed density functional theory (DFT) calculations, finding structures for SiC_6H_6^+ like those calculated by Schwarz and co-workers.¹⁰

Our research group has employed photodissociation mass spectrometry measurements to study a variety of metal ion–benzene complexes.¹⁸ In UV photodissociation experiments, metal ion–benzene complexes are found to dissociate primarily by ligand elimination, but metal-to-ligand charge transfer dissociation is often a prominent process. We have recently demonstrated the application of infrared photodissociation

* Corresponding author. E-mail: maduncan@uga.edu.

spectroscopy to metal–benzene ions to probe their vibrational spectroscopy for the first time in the gas phase.^{24–27} IR spectra in the fingerprint region were obtained using an infrared free-electron laser,^{24–26} while spectra in the C–H stretching region were obtained with an IR optical parametric oscillator (OPO) laser system.²⁷ In the present study, we employ both UV photodissociation and IR photodissociation spectroscopy in the C–H stretch region to investigate $\text{Si}^+(\text{C}_6\text{H}_6)_n$ complexes. These studies provide a new perspective on the structure and bonding in the silicon–benzene ion system.

Experimental Section

Clusters of the form $\text{Si}^+(\text{C}_6\text{H}_6)_n$, $\text{Si}^+(\text{C}_6\text{D}_6)_n$, and $\text{Si}^+(\text{C}_6\text{H}_6)\text{-Ar}$ are produced by laser vaporization in a pulsed nozzle cluster source and mass analyzed in a reflectron time-of-flight mass spectrometer.⁴¹ The third harmonic (355 nm) of a Nd:YAG laser (Spectra Physics INDI 30) is used to vaporize a rotating and translating silicon rod (ESPI). An argon expansion is seeded with benzene at ambient conditions using a General Valve (Series 9). The expansion is skimmed from the source chamber into the differentially pumped chamber where the ions are pulse-extracted into the time-of-flight mass spectrometer. Ions of interest are mass selected by pulsed deflection plates located near the end of the first drift tube section. The selected parent ion is photodissociated by intersecting the ion beam with a laser in the turning region of the reflectron field. Parent and fragment ions are mass analyzed in the second drift tube section and detected with an electron multiplier tube. For UV photodissociation, the third harmonic (355 nm) of a Nd:YAG laser (Spectra Physics DCR-11) is employed, with a pulse energy of about 20 mJ/cm²·pulse. Pulse energies are varied down to about 1 mJ/cm²·pulse to investigate multiphoton effects. Infrared experiments use an optical parametric oscillator/amplifier (OPO/OPA) system (LaserVision) pumped by a Continuum 9010 Nd:YAG laser. This system generates tunable IR in the 2000–4000 cm⁻¹ region. Photodissociation is enhanced on resonance with molecular vibrations of the ligand, and infrared photodissociation spectra are obtained by monitoring the fragment ion yield versus the IR wavelength. Wavelength calibration for the OPO is achieved using photoacoustic spectroscopy of methane, which has a well-known rotationally resolved C–H stretching band in the 3100 cm⁻¹ region. Band positions are accurate to within ± 1 cm⁻¹. Data are collected with a digital oscilloscope (LeCroy Waverunner LT-342) and transferred to a PC via an IEEE-488 interface.

Theoretical Methods

The structure, vibrational frequencies, and infrared oscillator strengths of the $\text{Si}^+(\text{C}_6\text{H}_6)$ complex were calculated using density functional theory with the Gaussian 03W program package.⁴² We employed the Becke-3 Lee–Yang–Parr (B3LYP) functional^{43,44} and the 6-311++G** basis set. The silicon cation was positioned initially near the C₆ axis of the benzene ring, but it was allowed to move to obtain the lowest energy structure. The primary interaction in the complex was believed to be electrostatic in nature, and hence the electronic states considered were those of the singly charged silicon cation. The vibrational frequencies of the different $\text{Si}^+(\text{C}_6\text{H}_6)$ isomers were scaled according to methods described previously for related systems when using the B3LYP/6-311++G** method.^{45,46} The scaling factors employed were 0.958 for the C–H stretching modes and 0.983 for the lower-frequency ring-based modes.

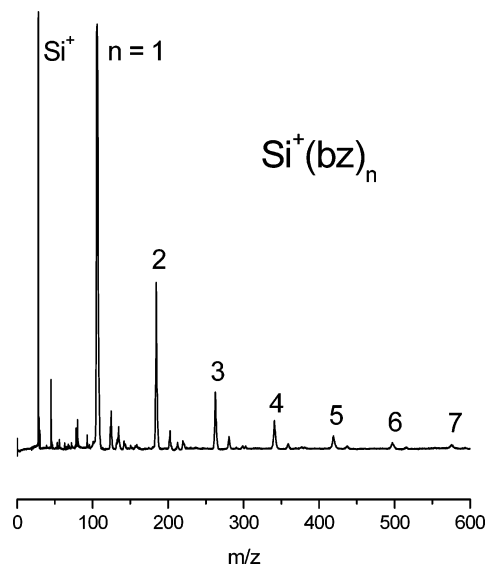


Figure 1. Mass spectrum for $\text{Si}^+(\text{benzene})_n$ clusters formed as ions directly from our cluster source. Next to the $\text{Si}^+(\text{benzene})_n$ cluster masses are peaks attributed to one or two water molecules clustering around the $\text{Si}^+(\text{benzene})_n$ clusters. There are also small signals for $\text{Si}_2^+(\text{benzene})_n$ clusters where $n = 1$ and 2.

Results and Discussion

The distribution of cluster ions produced directly from the laser vaporization source is presented in Figure 1. We employ a “cutaway” type rod holder with no gas channel beyond the laser vaporization point.⁴¹ This configuration provides efficient formation of cold cation–molecular complexes. Ions of the form $\text{Si}^+(\text{C}_6\text{H}_6)_n$ are produced efficiently for the $n = 1$ and 2 complexes, and clustering is evident up to the $n = 7$ cluster size. The relative intensity of the $n = 1$ complex is nearly the same as that of the silicon cation, and this is much greater than the intensity of the larger clusters. This demonstrates the ease with which a silicon cation forms an ion–molecule complex with benzene in the laser plasma, consistent with the results obtained by other research groups.^{7–9,12,15} Other minor mass peaks are attributed to SiOH^+ and $\text{Si}^+(\text{C}_6\text{H}_6)_n(\text{H}_2\text{O})_m$ complexes, resulting from a slight water impurity. The mass at 56 amu is Si_2^+ , and there are also peaks corresponding to $\text{Si}_2^+(\text{C}_6\text{H}_6)_n$ for $n = 1$ and 2. The benzene cation is detected, and there are other masses between Si^+ and $\text{Si}^+(\text{C}_6\text{H}_6)$ that are most likely caused by fragmentation of $\text{Si}^+(\text{C}_6\text{H}_6)$ complexes in the laser plasma. These include SiC_2H^+ , SiC_4H_3^+ , and SiC_5H_5^+ . The latter ion was also prevalent in the work of Tang and co-workers.¹⁵ These mass assignments were confirmed in experiments using C_6D_6 .

We next investigate photodissociation of these silicon-containing ions. Based on the previously calculated binding energies, photodissociation of $\text{Si}^+(\text{C}_6\text{H}_6)$ at visible or near-UV wavelengths should be energetic enough to break the Si^+ –benzene bond. However, virtually no such simple ligand cleavage process is observed. Instead, when $\text{Si}^+(\text{C}_6\text{H}_6)$ was photodissociated at 355 nm, the fragmentation pattern contained several $\text{Si}^+\text{C}_n\text{H}_m$ fragments and was nearly identical to the collisionally activated dissociation spectrum observed by Schwarz and co-workers.⁹ Unfortunately, our mass resolution was not sufficient to completely separate all the hydrogen-containing fragment ions. To clarify the situation, we performed the same experiment with C_6D_6 . Figure 2 shows the photodissociation mass spectrum of $\text{Si}^+(\text{C}_6\text{D}_6)$ at 355 nm. This photodissociation data is obtained by a difference method in which the spectrum with the laser “off” is subtracted from one with it “on”. The negative peak indicates depletion of the selected parent ion,

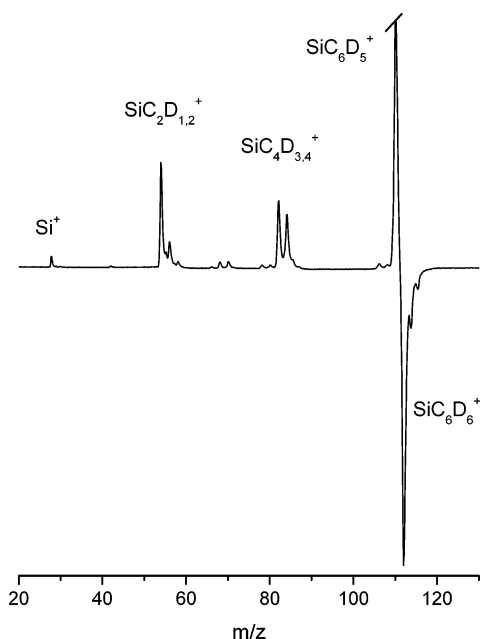


Figure 2. UV fixed frequency photodissociation of $\text{Si}^+(\text{C}_6\text{H}_6)$ at 355 nm. This type of spectrum is acquired by subtracting a mass spectrum of the selected parent ion from one with the photodissociation laser on. The resulting mass spectrum shows parent ion depletion as a negative peak and the fragment ions as positive peaks.

while the positive peaks indicate the photofragments. The main fragment ions detected are SiC_6D_5^+ , SiC_4D_4^+ , SiC_4D_3^+ , SiC_2D_2^+ , SiC_2D^+ , and Si^+ . Minor amounts of SiC_3D_3^+ , SiC_3D_2^+ , and C_4D_5^+ are also detected. There is a mass coincidence at 84 amu, and this peak could be assigned to either $\text{Si}^+\text{C}_4\text{D}_4$ or C_6D_6^+ . This coincidence should not occur for the fully hydrogenated benzene complex. However, in our data for that complex we detect a broad unresolved mass peak in this region, suggesting that C_6H_6^+ is probably formed, but precluding a clear assignment.

This fragmentation pattern indicates that there is significant decomposition of the benzene ring as the complex breaks apart. This behavior is quite different from the photodissociation processes measured previously for most *metal* ion–benzene complexes, where simple ligand elimination or charge transfer have been found.¹⁸ If there is a π -complex isomer, it might be expected to dissociate like these $\text{M}^+(\text{C}_6\text{H}_6)$ complexes. However, only a small amount of the Si^+ ion is detected here that might come from such a simple ligand elimination process. The ionization potential (IP) of silicon (8.15 eV)⁴⁷ is lower than that of benzene (9.24 eV),⁴⁸ and therefore ligand elimination would normally produce charged silicon and neutral benzene, consistent with the appearance of Si^+ . However, because of the low IP difference between Si and benzene, charge-transfer dissociation¹⁸ like that seen for many metal ion–benzene complexes might also occur for a π -complex. This would produce the C_6H_6^+ (or C_6D_6^+) ion. As noted above, resolution issues and mass coincidences make it impossible to confirm that the benzene molecular ion is detected. However, we can say that any such ions are present only in minor concentration. The most prominent fragment ion is SiC_6D_5^+ , which could easily be rationalized to come from an isomer with Si^+ inserted in a C–D bond. The other fragment ions SiC_4D_4^+ , SiC_4D_3^+ , SiC_3D_3^+ , SiC_3D_2^+ , SiC_2D_2^+ , and SiC_2D^+ could be rationalized to come from a ring insertion isomer. However, we must bear in mind that photodissociation can occur via significant structural rearrangements. The fact that the UV fragmentation channels measured here are exactly the same as those seen by previous

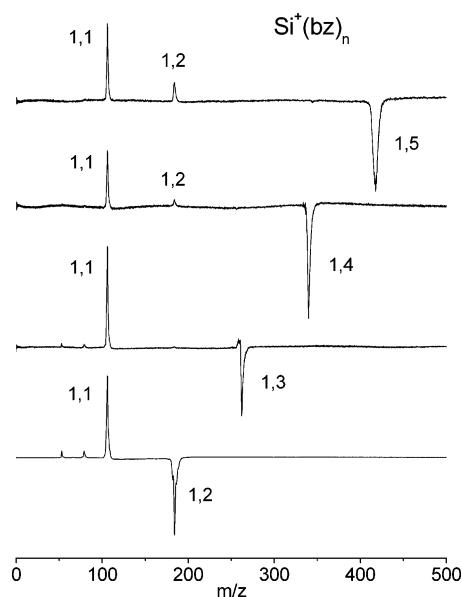


Figure 3. Photodissociation of $\text{Si}^+(\text{C}_6\text{H}_6)_n$ where $n = 2-5$ at 355 nm. All of the larger clusters produce the $\text{Si}^+(\text{C}_6\text{H}_6)$ species as the main fragment, but there is some tendency for the survival of the $n = 2$ species from the $n = 4$ and 5 parent ions.

collisional excitation indicates that the dissociation process occurs in the ground electronic state. UV photoexcitation is apparently followed by intramolecular internal conversion, producing hot ground-state molecules that undergo unimolecular fragmentation along the lowest energy channels. Dissociation in this way can proceed via extensive rearrangement processes. Therefore, the UV dissociation results here are consistent with any of the three isomeric structures proposed previously, but these results are not able to either rule out or confirm their presence.

Figure 3 shows the photodissociation of several larger $\text{Si}^+(\text{C}_6\text{H}_6)_n$ complexes. The dissociation of such larger complexes is often informative, because it allows determination of the coordination number of ligands around the core ion. Ligands bound directly to the core ion have relatively strong ion–ligand bonds via charge-dipole, charge-induced dipole, and other forces, while external ligands are bound primarily by much weaker van der Waals forces. Such external ligands would have binding energies roughly equivalent to that of the benzene dimer (about 1000 cm^{-1}).^{49–51} For example, UV photodissociation of various metal ion–benzene complexes, $\text{M}^+(\text{C}_6\text{H}_6)_n$ ($n = 3-8$) dissociate to produce the $\text{M}^+(\text{C}_6\text{H}_6)_2$ ion that is understood to represent the sandwich structure.^{18c} Similar fragmentation processes have identified the coordination number for other metal ion–ligand complexes.⁴¹ Surprisingly, the photodissociation mass spectra for the $n = 2-5$ silicon ion–benzene complexes do not terminate at the $n = 2$ species that would indicate a stable sandwich. Instead, these fragmentation processes terminate at the $\text{Si}^+(\text{C}_6\text{H}_6)$ ion. A small amount of $n = 2$ fragment ions is detected as a fragment from the $n = 4,5$ complexes. This suggests that $\text{Si}^+(\text{C}_6\text{H}_6)$ is the stable cluster size and other larger complexes have relatively lower binding energies. In particular, there is no indication at any cluster size for termination of ligand loss at the $n = 2$ sandwich species. Apparently, stable benzene sandwich species are not favored for a silicon cation. This result is consistent with the work of Dunbar and co-workers,¹² who also did not find any sandwich species under their conditions. It seems then that a single benzene molecule is closely associated with Si^+ in these complexes and that other benzene molecules are more weakly attached. We form these larger complexes in

our ion source, as did Tang and co-workers,¹⁵ because the supersonic expansion conditions stabilize even very weakly bound ions. Dunbar and others did not see larger complexes, most likely because their low pressure conditions could only stabilize more strongly bound species.

The lack of any stable sandwich structure for silicon–benzene complexes is perhaps understandable. In transition metal–benzene complexes, partially filled d orbitals are available for s–d hybridization and these orbitals undergo charge acceptance and donation interactions. By contrast, the first excited d atomic state for Si⁺ lies more than 9.8 eV higher in energy than the occupied 3p orbital.⁵² It is therefore understandable that hybridization is inefficient. Si⁺ therefore prefers to bind covalently and directionally with its s and p valence orbitals, and therefore it cannot interact effectively with two benzene ligands.

To further investigate the possibility of Si⁺(C₆H₆) isomers in our molecular beam, we employed infrared photodissociation spectroscopy on these ions. We focus this study in the region of the C–H stretch vibrations of benzene, near 3100 cm⁻¹.^{53,54} On the basis of the previously calculated binding energies,¹⁰ excitation into the C–H stretch region is not energetic enough to cause photodissociation of the Si⁺(C₆H₆) complex, except by inefficient multiphoton processes. Consistent with these energetics, we were not able to photodissociate the Si⁺(C₆H₆) complex with infrared excitation. To improve the efficiency of photodissociation, we use rare gas “tagging” with argon.^{41,55–59} For this experiment, we make the mixed complex Si⁺(C₆H₆)Ar and study its photodissociation spectrum. Argon is weakly bound so that it can enhance the photodissociation yield, while hopefully not adding any significant perturbation to the spectroscopy. Although the binding energy of Si⁺ to argon is not known, we observe relatively efficient photodissociation for the mixed ion in the 3100 cm⁻¹ region. Figure 4 shows the comparison of spectra for the Si⁺(C₆H₆)Ar, Si⁺(C₆H₆)₂, and Si⁺(C₆H₆)₃Ar ions in the 2900–3300 cm⁻¹ range. The spectrum for the Si⁺(C₆H₆)Ar and Si⁺(C₆H₆)₃Ar clusters were monitored in the loss of argon channel, while the spectra for the Si⁺(C₆H₆)₂ cluster was monitored in the loss of benzene channel.

The main feature in the Si⁺(C₆H₆)Ar spectrum is a single band centered at 3086 cm⁻¹, and there are additional shoulders and satellite structure nearby. Consistent with our previous work on metal ion–benzene complexes,²⁷ we do not see the Fermi triad here that is commonly seen in IR spectroscopy for liquid or gaseous benzene in the C–H stretch region.^{53,54} This Fermi triad comes from the e_{1u} frequencies of the ν₁₂ fundamental and the ν₁₃ + ν₁₆ and ν₂ + ν₁₃ + ν₁₈ combination bands, and its members occur at 3037, 3074, and 3093 cm⁻¹ for liquid benzene⁵³ and 3048, 3079, and 3101 cm⁻¹ for benzene in the gas phase.⁵⁴ The vibrations noted are accidentally degenerate in the free benzene molecule, but they are apparently shifted enough in the M⁺ and Si⁺ complexes to remove this degeneracy. In the present spectrum, there is a shoulder on the left side of this peak, suggesting the presence of more than one overlapping vibrational band, and there is a weak additional band at 3115 cm⁻¹. The dashed red line in the figure shows the position of the ν₁₂ vibration in gas-phase benzene. We have indicated the recommended frequency for the ν₁₂ mode (3063 cm⁻¹) that would be found without the Fermi resonance.⁵³ The main peak in the Si⁺(C₆H₆)Ar spectrum is located at 3086 cm⁻¹, which is then shifted 23 cm⁻¹ to the blue from the ν₁₂ vibration in benzene. We have recently reported a similar blue-shift for the IR spectrum of V⁺(C₆H₆)_n in the same C–H stretching region.²⁷

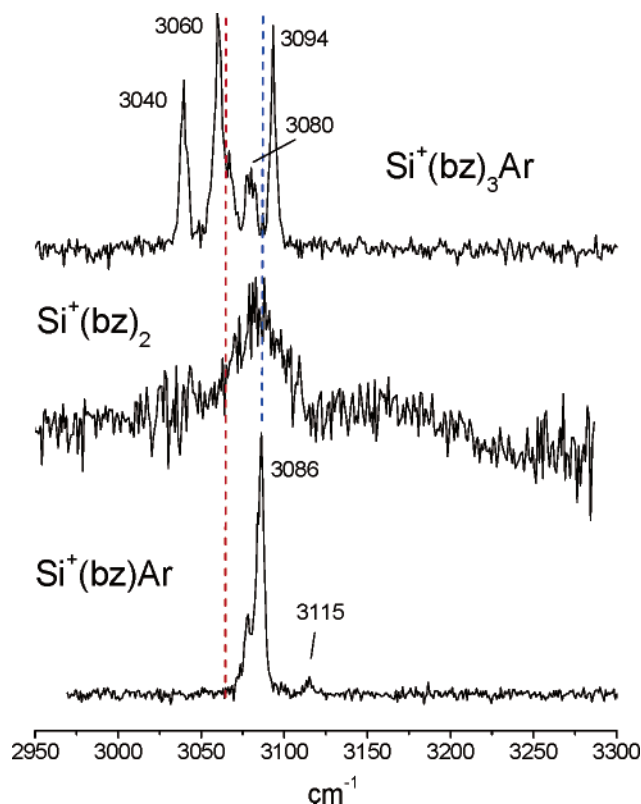


Figure 4. Infrared photodissociation spectra of Si⁺(C₆H₆)Ar, Si⁺(C₆H₆)₂, and Si⁺(C₆H₆)₃Ar. Spectra are acquired by monitoring the fragment ion (Ar loss for the “tagged” clusters and C₆H₆ loss for the *n* = 2 cluster) intensity versus the infrared frequency. The dashed line (to the left) indicates the rated frequency value of the ν₁₂ C–H stretch of free gas-phase benzene at 3063 cm⁻¹ in the absence of the Fermi triad. The other dashed line indicates the peak position of the “core” mode (free of solvation) for the Si⁺(C₆H₆)Ar cluster.

At first glance, a blue-shift for the C–H stretch vibration is surprising. The Dewar–Chatt–Duncanson complexation model, which is often applied to metal carbonyl complexes, is also usually applied to metal–benzene systems.^{60–62} In this model, the metal–ligand interaction is composed of σ-donation of ligand bonding electron density into empty metal orbitals and π back-bonding of metal electron density into the π*-antibonding orbitals of the ligand. Both of these effects weaken the bonding on the ligand framework and most often the vibrations are shifted to *lower* frequencies. In our studies of metal–benzene complexes in the fingerprint IR region,²⁶ we found that the ν₁₉ vibrations were indeed shifted significantly to the red. However, as we have noted before,²⁷ the C–H modes apparently behave differently. We can rationalize this behavior by comparing to a recent IR spectroscopy study performed by Dopfer and co-workers on the benzene cation (tagged in various ways).⁶³ This study found a blue-shift for the C–H stretches in the benzene cation compared to the neutral, that was attributed to a stiffening of the bonds because of loss of electron from the HOMO e_{1g} orbital of benzene. Apparently, when metal or Si⁺ ions bind to benzene, some charge transfer of electron density toward the cation takes place, leaving a partial charge on the benzene. This polarized ligand then behaves to some degree like the benzene cation, and the C–H stretches shift to higher frequency.

The Si⁺(C₆H₆)₂ cluster photodissociates inefficiently and its spectrum shows a broad band which appears to be centered at nearly the same position as that of the Si⁺(C₆H₆)Ar complex. We were unable to argon tag the *n* = 2 cluster to better resolve the peak position and increase the photodissociation yield.

Although the data is then unclear, we can say from the line width observed that there is probably no evidence for a Fermi triad in this spectrum. This suggests that the binding of the second ligand to Si^+ , while it may be much weaker than the first, is still able to shift benzene vibrations enough to remove the degeneracy found in the free molecule. The inefficient photodissociation for this cluster at the IR wavelengths suggests that the second benzene is bound by more than 3000 cm^{-1} . The small amount of the $n = 2$ fragment that survives in the UV photodissociation studies is also consistent with a somewhat stronger bonding in this cluster than for the larger ones.

For the $\text{Si}^+(\text{C}_6\text{H}_6)_3$ species, we are able to measure the spectrum with good intensity via the loss of benzene, and we are also able to tag this cluster with argon to measure it in the argon loss channel. The spectra measured in these two ways are identical, except that the signal level is better with tagging. The efficient photodissociation seen in the $\text{Si}^+(\text{C}_6\text{H}_6)_3$ spectrum without tagging is attributed to the presence of a benzene molecule interacting much more weakly with the silicon cation. Because dissociation occurs readily in the C–H stretching region of the IR, the last benzene in the cluster must be bound by less than about 3000 cm^{-1} . Figure 4 shows the spectrum for $\text{Si}^+(\text{C}_6\text{H}_6)_3\text{Ar}$. In this spectrum there is a marked change from those for the smaller cluster sizes. A multiplet of at least four bands are measured at 3040, 3060, 3080, and 3094 cm^{-1} . The band at 3080 cm^{-1} is at nearly the same position as the main band of the $\text{Si}^+(\text{C}_6\text{H}_6)\text{Ar}$ cluster (3086 cm^{-1}), and therefore we can assign it to be the same mode as in that so-called “core” ion. The other three bands have positions very close to the Fermi triad bands, which occur at 3037, 3074, and 3093 cm^{-1} for liquid benzene.⁵³ The positions of the outer two multiplet bands here in the $n = 3$ spectrum are each within 1–3 cm^{-1} of the liquid benzene triad bands, while the central more intense band at 3060 cm^{-1} is shifted 14 cm^{-1} to the red from the corresponding band in benzene. These three bands have comparable relative intensities, similar to the triad bands in benzene. Although the lines positions are not exactly the same, we believe that the triplet seen here should be associated with the C–H triad structure in benzene. This is therefore evidence for the presence of one benzene molecule that is essentially unperturbed compared to molecules in the liquid, that is, one that is not bound tightly to the silicon cation. This “external” molecule can then be regarded more as a “solvent” molecule in the cluster than as a ligand.

If the $n = 3$ complex has one external ligand, then larger complexes should have more external ligands. Figure 5 shows a comparison of the $n = 3$ and $n = 4$ spectra to the spectrum for liquid benzene taken from the NIST website.⁵³ The spectrum for $n = 4$ has a multiplet that is quite similar to that of the $n = 3$ species discussed above. The resemblance to the liquid benzene IR spectrum is again recognizable, although the line positions do not match exactly. The outer multiplet members appear again at 3040 and 3094 cm^{-1} , and are 1–3 cm^{-1} away from the corresponding liquid benzene triad bands. In the center of the multiplet, however, the $n = 4$ species has two peaks (3058 and 3069 cm^{-1}) instead of the one seen at 3060 for the $n = 3$ complex. Additionally, there is a reproducible shoulder at 3080 cm^{-1} that corresponds to the core vibration of the $n = 1$ species. It is not clear why the single central band for the $n = 3$ evolves to become a doublet for the $n = 4$ complex. It is conceivable that the two external benzene molecules in this complex are in slightly different bonding configurations, so that this band occurs at a slightly different frequency for each of these. Other assignments are also possible for the central bands in the multiplet (shifted core peaks, etc.). However, the close cor-

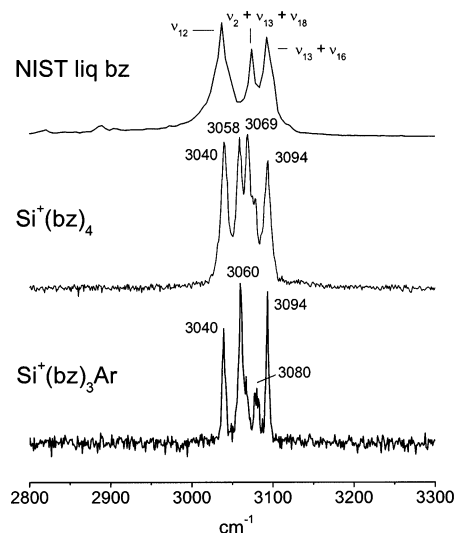


Figure 5. IR photodissociation spectra for $\text{Si}^+(\text{C}_6\text{H}_6)_n\text{Ar}$ and $\text{Si}^+(\text{C}_6\text{H}_6)_4$ compared to the Fermi triad in liquid benzene.

respondence of the outer multiplet members to the triad spectrum suggests that the additional benzenes for the $n = 3$ and $n = 4$ complexes both represent molecules that are only slightly perturbed compared to free benzene. This information and the ease of eliminating these molecules by IR photodissociation are both consistent with the assignment of these benzene molecules as more solvent-like than ligand-like.

The overall picture of ligand binding in the $\text{Si}^+(\text{C}_6\text{H}_6)_n$ system, therefore, is that the first benzene molecule is bound strongly to the cation, and this complex forms a core ion with a spectrum quite different from that of benzene itself. The $n = 2$ complex has one strongly bound benzene and one less strongly bound benzene. The second ligand is bound strongly enough to have a perturbed spectrum, to exhibit inefficient dissociation in the IR, and to survive in small amounts in some of the UV dissociation studies. The additional benzene in the $n = 3$ and $n = 4$ complexes are weakly bound and have spectra like those of liquid benzene, indicating that they can be regarded as solvent species rather than ligands.

To examine the structure of the $\text{Si}^+(\text{C}_6\text{H}_6)$ cluster in more detail, and to investigate the possibility of structural isomers for this species, we performed DFT calculations on this complex. The results of these calculations are presented in Figure 6 and Table 1. As shown in Figure 6, we located three isomeric structures and found each to be a minimum on the potential surface. The qualitative details of the structures calculated for $\text{Si}^+(\text{C}_6\text{H}_6)$ are the same as those found by the Schwarz and Tang groups.^{10,15} They can be identified as the π -complex, the C–H inserted isomer, and the ring-inserted isomer, respectively. Consistent with the results of Schwarz, we found the π -complex to lie significantly lower in energy than the inserted structures. The silicon ion in this isomer is positioned away from the C_6 axis of the benzene ring in a site located nearly above one carbon of the benzene ring. The nearest hydrogen atom is bent out of the plane of the benzene ring by about 10 degrees. The insertion complexes have the silicon in a $\text{C}_6\text{H}_5\text{—Si—H}$ position or in a seven-membered ring with the six carbon atoms. Previous theoretical studies did not report vibrational frequencies for these different isomers, and therefore we use our calculations to determine these.

Figure 7 shows the comparison between the calculated vibrational frequencies for each of the different isomers of $\text{Si}^+(\text{C}_6\text{H}_6)$ and the experimental spectrum acquired for $\text{Si}^+(\text{C}_6\text{H}_6)\text{—Ar}$. In each structure, there is significantly lowered symmetry

TABLE 1: Binding Energies (relative to separated Si⁺ and benzene) and Vibrational Frequencies Calculated for the Different Si⁺(C₆H₆) Isomers

structure	B.E. (kcal/mol)	IR frequency ^a (IR intensity (km/mol))
π -complex	-51.2	3081 (5), 3067 (12), 3065 (6), 3060 (4), 3052 (3), 3049 (0.2), 1548 (20), 1528 (7), 1467(34), 1457 (39), 1353 (0.4), 1274 (0.3), 1180 (8), 1144 (0.5), 1030 (1), 1017(0.0), 1001 (0.8)
Si-H insertion	-46.1	3073 (0.2), 3067 (0.7), 3056(0.5), 3049 0.4), 3042 (0.9), 2130 (13), 1578 (98), 1551 (4.5), 1470 (0.1), 1432 (44), 1346 (18), 1291 (3), 1198 (6), 1183 (3), 1094 (4), 1081 (103), 1021 (0.4), 1018 (2)
ring insertion	-37.9	3044 (0.5), 3031 (7), 3029(5), 3027 (5), 3001 (2), 3000 (0.2), 1582 (1), 1530 (0.8), 1493 (57), 1472 (18), 1378 (81), 1358 (3), 1315 (5), 1246 (4), 1208 (0.2), 1038 (4), 1019 (0.0), 1018 (0.0), 1002 (0.0)

^a The scaling factor is 0.958 for the C-H modes and 0.983 for the lower frequencies.

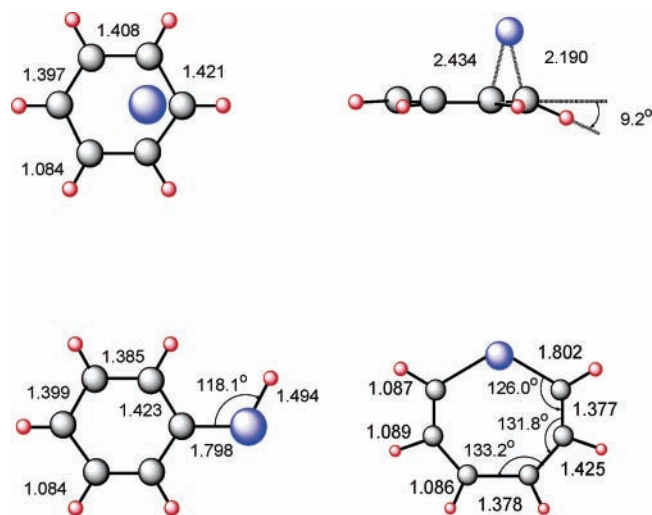


Figure 6. The isomeric structures calculated via DFT for the SiC₆H₆⁺ complex. The upper two structures provide different views of the π -complex, while the lower two structures are the respective insertion isomers.

compared to benzene itself, and therefore there is a multiplet of IR-active vibrational modes predicted in the C-H stretching region. The frequencies and their IR intensities are given in Table 1. The predicted IR spectrum for each isomer differs in the relative intensity pattern distributed across the multiplet of modes in this region. These multiplets are indicated in different colors in Figure 7. The C-H inserted isomer spectrum looks the least like the experimental spectrum. It has five bands with almost equal intensity distributed across a range of about 30 cm⁻¹, while the experimental spectrum consists of one main band much narrower than this. Additionally, this isomer is predicted to have an Si-H stretch vibration near 2130 cm⁻¹ with much stronger IR intensity than the modes in the C-H stretch region. We scanned this region and found no signal within our detection limits. We can therefore safely eliminate the C-H insertion isomer as a candidate for the SiC₆H₆⁺ structure. The ring-insertion isomer has most of its IR bands clustered into a group, and these could appear to be a single peak in a spectrum with our resolution. However, the resonances are predicted to lie near 3030 cm⁻¹, while our band is found at 3086 cm⁻¹. Additionally, there is an additional single band predicted with good IR intensity shifted even farther to the red near 3000 cm⁻¹. We do not see any evidence for a red satellite band in our spectrum. These details make it seem unlikely that the ring-insertion isomer is present. The best agreement between

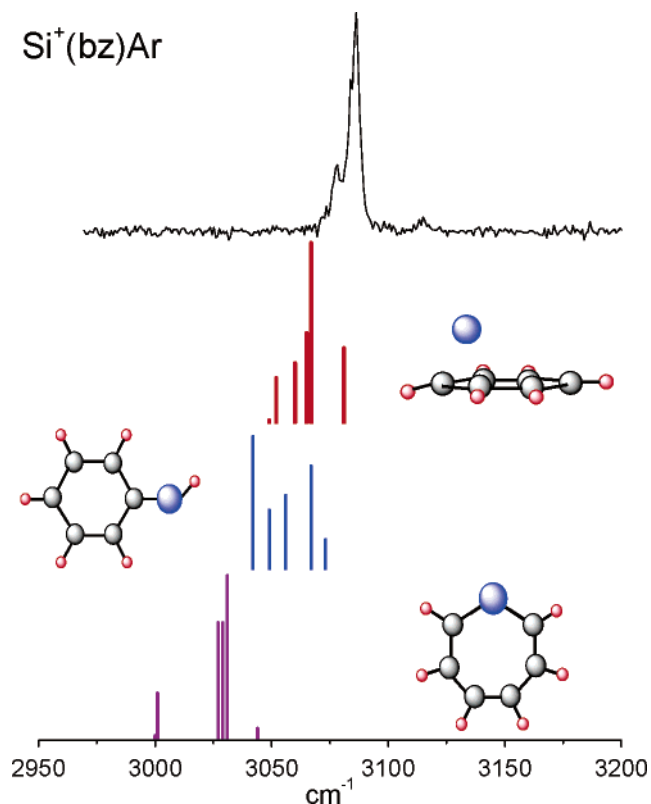


Figure 7. Comparison of the Si⁺(C₆H₆)Ar spectrum obtained experimentally versus the vibrational frequencies calculated by B3LYP/6-311++G** for the different isomers. The experimental spectrum agrees best with that of the π -complex.

theory and experiment is found for the π -complex. This isomer has most of its IR bands in the 3060–3080 region of the spectrum, with the most intense features lying within about 20 cm⁻¹ of the experimental band position. Additionally, less intense bands are predicted to the red of the main band, consistent with the red shading and shoulder features seen in the experiment. Finally, a weak blue-shifted satellite band is predicted for this isomer about 20 cm⁻¹ to the blue of the main band, and we observe such a satellite band at 3115 cm⁻¹ that is about 30 cm⁻¹ to the blue from our main band. We should note here that the theory we have done is for the Si⁺(C₆H₆) complex, while the experiment is for the argon-tagged species, and some slight shifts could be caused by the argon. However, if we consider both the absolute frequency positions and the distribution of the allowed IR bands, it is clear that there is very good

agreement between the spectrum predicted for the π -complex and the experimental spectrum. The π -complex is also the one predicted by theory to be most stable, and by inspection it is also least likely to have an activation barrier in its formation path. We therefore conclude that our infrared experiment has measured the spectrum for the π -complex.

It is important to note that we cannot rule out the presence of the one or both of the other isomers in minor concentrations. The IR bands predicted in the C–H stretching region are more intense for the π -complex than they are for the other isomers, and therefore this species would be easier to detect. The lack of any resonance near 2130 cm^{-1} argues strongly against any major component of the Si–H insertion isomer, but the ring-insertion isomer has only very weak intensity bands predicted throughout the region of the experiment. Concentrations of this isomer that are 3–5 times less than the π -complex would almost certainly be missed by our experiment because of our limited sensitivity. Future experiments may be able to probe these complexes in the region of the ring distortion vibrations (1300 – 1500 cm^{-1}) where much more intense vibrations are predicted for all three isomers. These experiments could provide a more stringent test for the presence, if any, of the minor isomers. It is also worth noting that the isomers not detected here could be present in other experiments because of the different ion sources employed. The laser ablation method that we use is relatively gentle and does not lead to extensive rearrangements of the ions. Condensation also occurs at low temperature in a supersonic expansion. It will therefore be interesting in future experiments to combine the IR methods described here with other ion production schemes to investigate this and other cluster isomer issues.

Conclusion

We report here the first study of the photodissociation behavior of $\text{Si}^+(\text{C}_6\text{H}_6)_n$ complexes. UV photodissociation experiments at 355 nm probe the decomposition pathways of these ions, while infrared experiments in the C–H stretching region investigate structural isomers that have been predicted by theory. On the basis of the results of both UV and IR photodissociation, we find that the mono-ligand complex is significantly more strongly bound than larger complexes. The second benzene is somewhat less strongly associated than the first in the $n = 2$ complex, and then additional benzenes beyond this are weakly bound and may be regarded as solvent.

The spectrum of the $\text{Si}^+(\text{C}_6\text{H}_6)\text{Ar}$ complex yields an asymmetric band centered at 3086 cm^{-1} with additional structure coming from shoulders and weaker satellite bands. A comparison to the predictions of theory shows that these band positions and their intensity distributions are in very good agreement with those predicted for the π -complex isomer. Our limited sensitivity prevents us from ruling out the presence of other isomers, but their concentration, if any, in the experiment must be significantly less than that of the π -complex.

Acknowledgment. We acknowledge generous support for this work from the National Science Foundation (Grant CHE-0244143).

References and Notes

- (1) Ferguson, E. E.; Fahey, D. W.; Fehsenfeld, F. C.; Allbritton, D. L. *Planet Space Sci.* **1975**, *23*, 1621.
- (2) Atreya, S. K.; Pollack, J. B.; Matthews, M. S. *Origin and Evolution of Planetary and Satellite Atmospheres*; University of Arizona Press: Tucson, 1989.
- (3) Turner, J. L.; Dalgarno, A. *Space Sci.* **1977**, *213*, 386.

- (4) Millar, J. *Astrophys. Space Sci.* **1980**, *72*, 509.
- (5) Clegg, R. E. S.; van Ijzendoorn, L. J.; Allamandola, L. J. *Mon. Not. R. Astron. Soc.* **1983**, *203*, 125.
- (6) (a) Powell, M. J.; Easton, B. C.; Hill, O. F. *Appl. Phys. Lett.* **1981**, *38*, 794. (b) Meiners, L. G. *J. Vac. Sci. Technol.* **1982**, *21*, 655. (c) Lucovsky, G.; Richard, P. D.; Tsu, D. V.; Lin, S. Y.; Markunas, R. J. *J. Vac. Sci. Technol.* **1986**, *A4*, 681. (d) Kushner, M. J. *J. Appl. Phys.* **1988**, *63*, 2532.
- (7) (a) Allen, W. N.; Lampe, F. W. *J. Chem. Phys.* **1976**, *65*, 3378. (b) Allen, W. N.; Lampe, F. W. *J. Am. Chem. Soc.* **1977**, *99*, 2943. (c) Lim, K. P.; Lampe, F. W. *J. Chem. Phys.* **1992**, *96*, 2819.
- (8) (a) Boo, B. H.; Armentrout, P. B. *J. Am. Chem. Soc.* **1987**, *109*, 3549. (b) Boo, B. H.; Elkind, J. L.; Armentrout, P. B. *J. Am. Chem. Soc.* **1990**, *112*, 2083. (c) Boo, B. H.; Armentrout, P. B. *J. Am. Chem. Soc.* **1991**, *113*, 6401. (d) Kickel, B. L.; Fisher, E. R.; Armentrout, P. B. *J. Phys. Chem.* **1992**, *96*, 2603.
- (9) (a) Bohme, D. K.; Wlodek, S.; Wincel, H. *Astrophys. J.* **1989**, *342*, L91. (b) Bohme, D. K.; Wlodek, S.; Wincel, H. *J. Am. Chem. Soc.* **1991**, *113*, 6396. (c) Bohme, D. K. *Advances in Gas-Phase Ion Chemistry*; JAI Press Inc: Greenwich, 1992.
- (10) Srinivas, R.; Hrusak, J.; Sulzle, D.; Bohme, D. K.; Schwarz, H. *J. Am. Chem. Soc.* **1992**, *114*, 2802.
- (11) Nagano, Y.; Murthy, S.; Beauchamp, J. L. *J. Am. Chem. Soc.* **1993**, *115*, 10805.
- (12) (a) Dunbar, R. C.; Uechi, G. T.; Asamoto, B. *J. Am. Chem. Soc.* **1994**, *116*, 2466. (b) Pozniak, B. P.; Dunbar, R. C. *J. Am. Chem. Soc.* **1997**, *119*, 10439.
- (13) (a) Glosik, J.; Zakouril, P.; Skalsky, V.; Lindinger, W. *Int. J. Mass Spectrom. Ion Processes* **1995**, *149/150*, 499. (b) Glosik, J.; Zakouril, P.; Lindinger, W. *Int. J. Mass Spectrom. Ion Processes* **1995**, *145*, 155. (c) Glosik, J.; Zakouril, P.; Lindinger, W. *J. Chem. Phys.* **1995**, *103*, 6490.
- (14) Luder, Ch.; Georgiou, E.; Velegrakis, M. *Int. J. Mass Spectrom. Ion Processes* **1996**, *153*, 129.
- (15) Xing, X.; Tian, Z.; Liu, H.; Tang, Z. *Rapid Commun. Mass Spectrom.* **2003**, *17*, 1743.
- (16) Olkhov, R. V.; Nizkorodov, S. A.; Dopfer, O. *Chem. Phys.* **1998**, *239*, 393.
- (17) Jaeger, J. B.; Jaeger, T. D.; Brinkmann, N. R.; Schaefer, H. F.; Duncan, M. A. *Can. J. Chem.* **2004**, *82*, 934.
- (18) (a) Willey, K. F.; Cheng, P. Y.; Bishop, M. B.; Duncan, M. A. *J. Am. Chem. Soc.* **1991**, *113*, 4721. (b) Willey, K. F.; Yeh, C. S.; Robbins, D. L.; Duncan, M. A. *J. Phys. Chem.* **1992**, *96*, 9106. (c) Jaeger, T. D.; Duncan, M. A. *Int. J. Mass Spectrom.* **2005**, *241*, 165.
- (19) (a) Chen, Y. M.; Armentrout, P. B. *Chem. Phys. Lett.* **1993**, *210*, 123. (b) Armentrout, P. B.; Hales, D. A.; Lian, L. *Advances in Metal Semiconductor Clusters*; JAI Press: Greenwich, 1994. (c) Meyer, F.; Khan, F. A.; Armentrout, P. B. *J. Am. Chem. Soc.* **1995**, *117*, 9740. (d) Rogers, M. T.; Armentrout, P. B. *Mass Spectrom. Rev.* **2000**, *19*, 215.
- (20) Weis, P.; Kemper, P. R.; Bowers, M. T. *J. Phys. Chem. A* **1997**, *101*, 8207.
- (21) (a) Hoshino, K.; Kurikawa, T.; Takeda, H.; Nakajima, A.; Kaya, K. *J. Phys. Chem.* **1995**, *99*, 3053. (b) Judai, K.; Hirano, M.; Kawamata, H.; Yabushita, S.; Nakajima, A.; Kaya, K. *Chem. Phys. Lett.* **1997**, *270*, 23. (c) Yasuike, T.; Nakajima, A.; Yabushita, S.; Kaya, K. *J. Phys. Chem. A* **1997**, *101*, 5360. (d) Kurikawa, T.; Takeda, H.; Hirano, M.; Judai, K.; Arita, T.; Nagoa, S.; Nakajima, A.; Kaya, K. *Organometallics* **1999**, *18*, 1430. (e) Nakajima, A.; Kaya, K. *J. Phys. Chem. A* **2000**, *104*, 176.
- (22) (a) Dunbar, R. C.; Klippenstein, S. J.; Hrusak, J.; Stöckigt, D.; Schwartz, H. *J. Am. Chem. Soc.* **1996**, *118*, 5277. (b) Ho, Y. P.; Yang, Y. C.; Klippenstein, S. J.; Dunbar, R. C. *J. Phys. Chem. A* **1997**, *101*, 3338.
- (23) (a) Cabarcos, O. M.; Weinheimer, C. J.; Lisy, J. M. *J. Chem. Phys.* **1998**, *108*, 5151. (b) Cabarcos, O. M.; Weinheimer, C. J.; Lisy, J. M. *J. Chem. Phys.* **1999**, *110*, 8429.
- (24) van Heijnsbergen, D.; von Helden, G.; Meijer, G.; Maitre, P.; Duncan, M. A. *J. Am. Chem. Soc.* **2002**, *124*, 1562.
- (25) van Heijnsbergen, D.; Jaeger, T. D.; von Helden, G.; Meijer, G.; Duncan, M. A. *Chem. Phys. Lett.* **2002**, *364*, 345.
- (26) Jaeger, T. D.; van Heijnsbergen, D.; Klippenstein, S. J.; von Helden, G.; Meijer, G.; Duncan, M. A. *J. Am. Chem. Soc.* **2004**, *126*, 10981.
- (27) Jaeger, T. D.; Pillai, E. D.; Duncan, M. A. *J. Phys. Chem. A* **2004**, *108*, 6605.
- (28) Judai, K.; Sera, K.; Amatsutsumi, S.; Yagi, K.; Yasuike, T.; Nakajima, A.; Kaya, K. *Chem. Phys. Lett.* **2001**, *334*, 277.
- (29) Gerhards, M.; Thomas, O. C.; Nilles, J. M.; Zheng, W.-J.; Bowen, K. H., Jr. *J. Chem. Phys.* **2002**, *116*, 10247.
- (30) Li, Y.; Baer, T. *J. Phys. Chem. A* **2002**, *106*, 9820.
- (31) Bauschlicher, C. W.; Partridge, H.; Langhoff, S. R. *J. Phys. Chem.* **1992**, *96*, 3273.
- (32) Stöckigt, D. *J. Phys. Chem. A* **1997**, *101*, 3800.
- (33) (a) Yang, C.-N.; Klippenstein, S. J. *J. Phys. Chem.* **1999**, *103*, 1094. (b) Klippenstein, S. J.; Yang, C.-N. *Int. J. Mass Spectrom. Ion Processes* **2000**, *201*, 253.
- (34) Chaquin, P.; Costa, D.; Lepetit, C.; Che, M. *J. Phys. Chem. A* **2001**, *105*, 4541.

- (35) Pandey, R.; Rao, B. K.; Jena, P.; Blanco, M. A. *J. Am. Chem. Soc.* **2001**, *123*, 3799.
- (36) Kaczorwska, M.; Harvey, J. N. *Phys. Chem. Chem. Phys.* **2002**, *4*, 5227.
- (37) (a) Leger, A.; d'Hendecourt, L. B. *Astron. Astrophys.* **1985**, *146*, 81. (b) Allamandola, L. J.; Tielens, A. G. G. M.; Barker, J. R. *Astrophys. J. Lett.* **1985**, *290*, L25.
- (38) (a) van der Zwet, G. P.; Allamandola, L. J. *Astron. Astrophys.* **1985**, *146*, 76. (b) Crawford, M. K.; Tielens, A. G. G. M.; Allamandola, L. J. *Astrophys. J. Lett.* **1985**, *293*, L45.
- (39) Duley, W. W.; Jones, A. P. *Astrophys. J. Lett.* **1990**, *351*, L49.
- (40) Omont, A. *Astron. Astrophys.* **1986**, *164*, 159.
- (41) Duncan, M. A. *Int. Rev. Phys. Chem.* **2003**, *22/2*, 407.
- (42) Frisch, M. J.; Trucks, G. W.; Schlegel, H. B.; Scuseria, G. E.; Robb, M. A.; Cheeseman, J. R.; Montgomery, J. A., Jr.; Vreven, T.; Kudin, K. N.; Burant, J. C.; Millam, J. M.; Iyengar, S. S.; Tomasi, J.; Barone, V.; Mennucci, B.; Cossi, M.; Scalmani, G.; Rega, N.; Petersson, G. A.; Nakatsuji, H.; Hada, M.; Ehara, M.; Toyota, K.; Fukuda, R.; Hasegawa, J.; Ishida, M.; Nakajima, T.; Honda, Y.; Kitao, O.; Nakai, H.; Klene, M.; Li, X.; Knox, J. E.; Hratchian, H. P.; Cross, J. B.; Adamo, C.; Jaramillo, J.; Gomperts, R.; Stratmann, R. E.; Yazyev, O.; Austin, A. J.; Cammi, R.; Pomelli, C.; Ochterski, J. W.; Ayala, P. Y.; Morokuma, K.; Voth, G. A.; Salvador, P.; Dannenberg, J. J.; Zakrzewski, V. G.; Dapprich, S.; Daniels, A. D.; Strain, M. C.; Farkas, O.; Malick, D. K.; Rabuck, A. D.; Raghavachari, K.; Foresman, J. B.; Ortiz, J. V.; Cui, Q.; Baboul, A. G.; Clifford, S.; Cioslowski, J.; Stefanov, B. B.; Liu, G.; Liashenko, A.; Piskorz, P.; Komaromi, I.; Martin, R. L.; Fox, D. J.; Keith, T.; Al-Laham, M. A.; Peng, C. Y.; Nanayakkara, A.; Challacombe, M.; Gill, P. M. W.; Johnson, B.; Chen, W.; Wong, M. W.; Gonzalez, C.; Pople, J. A. *Gaussian 03 (Revision B.02)*; Gaussian, Inc.: Pittsburgh, PA, 2003.
- (43) Becke, A. J. *Chem. Phys.* **1993**, *98*, 5648.
- (44) Lee, C.; Yang, W.; Parr, R. G. *Phys. Rev. B* **1988**, *37*, 785.
- (45) Michalska, D.; Zierkiewicz, W.; Bienko, D. C.; Wojciechowski, W.; Zeegers-Huyskens, T. *J. Phys. Chem. A* **2001**, *105*, 8734.
- (46) (a) Baker, J.; Jarzecki, A. A.; Pulay, P. J. *J. Phys. Chem. A* **1998**, *102*, 1412. (b) Rauhut, G.; Pulay, P. *J. Phys. Chem. A* **1995**, *99*, 3095.
- (47) Lide, D. R. *Handbook of Chem. & Phys.*, 75th ed.; CRC: Boca Raton, FL, 1994.
- (48) Nemeth, G. I.; Selzle, H. L.; Schlag, E. W. *Chem. Phys. Lett.* **1993**, *215*, 151.
- (49) Grover, J. R.; Walters, E. A.; Hui, E. T. *J. Phys. Chem.* **1987**, *91*, 3233.
- (50) Krause, H.; Ernstberger, B.; Neusser, H. J. *Chem. Phys. Lett.* **1991**, *184*, 411.
- (51) Sinnokrot, M. O.; Valeev, E. F.; Sherrill, C. D. *J. Am. Chem. Soc.* **2002**, *124*, 10887.
- (52) Sansonetti, J. E.; Martin, W. C. *Handbook of Basic Atomic Spectroscopic Data*; NIST Physics Laboratory, Physical Reference Data, National Institute of Standards and Technology, Gaithersburg, MD 20899 (<http://physics.nist.gov>).
- (53) Shimanouchi, T. *Molecular Vibrational Frequencies*; NIST Chemistry WebBook, NIST Standard Reference Database Number 69, National Institute of Standards and Technology, Gaithersburg, MD 20899; July 2001 (<http://webbook.nist.gov>).
- (54) Snavely, D. L.; Walters, V. A.; Colson, S. D.; Wiberg, K. B. *Chem. Phys. Lett.* **1984**, *103*, 423.
- (55) (a) Okumura, M.; Yeh, L. I.; Lee, Y. T. *J. Chem. Phys.* **1985**, *83*, 3705. (b) Okumura, M.; Yeh, L. I.; Lee, Y. T. *J. Chem. Phys.* **1988**, *88*, 79.
- (56) (a) Meuwly, M.; Nizkorodov, S. A.; Maier, J. P.; Bieske, E. J. *J. Chem. Phys.* **1996**, *104*, 3876. (b) Dopfer, O.; Roth, D.; Maier, J. P. *J. Phys. Chem. A* **2000**, *104*, 11702. (c) Bieske, E. J.; Dopfer, O. *Chem. Rev.* **2000**, *100*, 3963.
- (57) (a) Ayotte, P.; Weddle, G. H.; Kim, J.; Johnson, M. A. *J. Am. Chem. Soc.* **1998**, *120*, 12361. (b) Ayotte, P.; Weddle, G. H.; Kim, J.; Johnson, M. A. *Chem. Phys.* **1998**, *239*, 485. (c) Ayotte, P.; Bailey, C. G.; Kim, J.; Johnson, M. A. *J. Chem. Phys.* **1998**, *108*, 444. (d) Nielson, S. B.; Ayotte, P.; Kelley, J. A.; Johnson, M. A. *J. Chem. Phys.* **1999**, *111*, 9593. (e) Corcelli, S. A.; Kelley, J. A.; Tully, J. C.; Johnson, M. A. *J. Phys. Chem. A* **2002**, *106*, 4872. (f) Robertson, W. H.; Johnson, M. A. *Annu. Rev. Phys. Chem.* **2003**, *54*, 173.
- (58) Pino, T.; Boudin, N.; Brechignac, P. *J. Chem. Phys.* **1999**, *111*, 7337.
- (59) Satink, R. G.; Piest, H.; von Helden, G.; Meijer, G. *J. Chem. Phys.* **1999**, *111*, 10750.
- (60) Chatt, J.; Rowe, G. A.; Williams, A. A. *Proc. Chem. Soc.* **1957**, 208.
- (61) Chatt, J.; Duncanson, L. A.; Guy, R. G. *J. Chem. Soc.* **1961**, 827.
- (62) Chatt, J.; Duncanson, L. A.; Guy, R. G.; Thompson, D. T. *J. Chem. Soc.* **1963**, 5170.
- (63) Dopfer, O.; Olkhov, R. V.; Maier, J. P. *J. Chem. Phys.* **1999**, *111*, 10754.